Journal of Structural Biology 174 (2011) 485–493

Contents lists available at ScienceDirect

Journal of Structural Biology

journal homepage: www.elsevier.com/locate/yjsbi

# Structure of a NADPH-dependent blue fluorescent protein revealed the unique role of Gly176 on the fluorescence enhancement

Tzu-Huei Kao [a,b], Yeh Chen [a,b], Chien-Hua Pai [a], Ming-Chung Chang [c], Andrew H.-J. Wang [a,b,*]

[a] Institute of Biological Chemistry, Academia Sinica, Taipei 115, Taiwan
[b] Core Facilities for Protein Production and X-ray Structural Analysis, Academia Sinica, Taipei 115, Taiwan
[c] Institute of Basic Medical Sciences, College of Medicine, National Cheng Kung University, Tainan 701, Taiwan

ARTICLE INFO

*Article history:*
Received 15 December 2010
Received in revised form 25 February 2011
Accepted 28 February 2011
Available online 10 March 2011

*Keywords:*
NADPH-dependent fluorescent protein
Blue fluorescent protein
Short-chain dehydrogenase/reductase
X-ray crystallography
Förster resonance energy transfer

ABSTRACT

A NADPH-dependent blue fluorescent protein from *Vibrio vulnificus* CKM-1 (BFPvv) emits blue fluorescence under UV-exposure. Previously, the BFPvvD7 mutant generated by directed evolution displayed a fourfold enhancement in fluorescent intensity. Herein, a further increase in fluorescence in the new BFPvvD8 mutant, with three additional mutations from BFPvvD7, was made. To understand the underlying mechanism of the increased fluorescent intensity of BFPvv, we solved the BFPvvD8-NADPH complex structure. Accompanied with lifetime detection, we proposed that the enhanced intensity is related to the conformational change caused by a glycine residue (Gly176) mutated to other non-glycine residues at a turn close to the NADPH binding site. We also observed the Förster resonance energy transfer (FRET) from our BFPvvD8 to each of the GFP-like fluorescent proteins, mTFP1 and EGFP, joined by an eight-residue linker between the N-terminal of BFPvvD8 and the C-terminal of GFPs. Taken together, with the newly solved BFPvvD8 structure, our results not only provide new considerations within the rational-based protein engineering of this NADPH-dependent BFP, but also suggest that BFPvvD8 could be a potential candidate in FRET-based biosensor techniques.



## 1. Introduction

The intramolecular chromophore formation of all GFP-like fluorescent proteins (FPs) requires the spontaneous oxygen-dependent cyclization steps (Heim et al., 1994); therefore, their usages are restricted to aerobic systems. In contrast, a different kind of FPs that capture certain prosthetic chromophore such as the oxygen-independent FMN-based fluorescent proteins (Drepper et al., 2007) and the infrared fluorescent proteins (IFP) (Shu et al., 2009) complements the biological applications of FPs.

Previously, a novel NADPH-dependent blue fluorescent protein BFPvv was discovered in *Vibrio vulnificus* CKM-1 (Su et al., 2001). BFPvv belongs to the short-chain dehydrogenase/reductase (SDR) family. This protein emits naked-eye detectable blue fluorescence under UV-exposure (Su et al., 2001), and its enzymatic activity was also detected by Polizzi et al. (2007). Furthermore, a BFPvv mutant, i.e., BFPvvD7, showed a fourfold increase of fluorescent intensity was derived via error-prone PCR (random mutagenesis) and DNA shuffling (Chang et al., 2004), with the rationales behind remain unclear. Previous studies among the fluorescent proteins demonstrated that how the fluorescence could be influenced by the surrounding environment in protein (Brejc et al., 1997). Knowledge about the structures of these proteins shall therefore provide useful information on the improvement of the FPs for applications.

Herein, we describe the discovery of another BFPvv mutant with further enhanced fluorescent intensity, called D8, caused by three additional mutations. The structure of this mutant was solved to a resolution of 2.05 Å. Through this structure information and other supporting data, we propose that the mutation of Gly176 to serine or alanine plays an important role in the fluorescence enhancement. Our results here provide new ideas for further protein engineering of this interesting BFP.

## 2. Material and methods

### 2.1. Protein expression and purification

The original WT BFPvv and BFPvvD8 coded pET21 expression vector were described previously (Chang et al., 2004). By using

*Abbreviations:* FP, fluorescent protein; BFP, blue fluorescent protein; GFP, green fluorescent protein; IFP, infrared fluorescent protein; NADPH, nicotinamide adenine dinucleotide phosphate reduced form; FMN, riboflavin mononucleotide; PCR, polymerase chain reaction; FRET, Förster resonance energy transfer; SDR, short-chain dehydrogenase/reductase; CAD, clavulanic acid dehydrogenase; WT, wild type; hCBR1, human carbonyl reductase 1.

* Corresponding author. Address: Institute of Biological Chemistry, Academia Sinica, 128, Academia Road, Section 2, Nankang, Taipei 11529, Taiwan. Fax: +886 2 2788 2043.
*E-mail address:* ahjwang@gate.sinica.edu.tw (A.H.-J. Wang).

1047-8477/$ - see front matter © 2011 Elsevier Inc. All rights reserved.
doi:10.1016/j.jsb.2011.02.010

BL21 (DE3) as the host cell, overexpression of each mutant was initiated by the addition of 1 mM IPTG under the incubation at 20 °C for 20 h. These recombinant proteins were collected and purified by using the $Ni^{2+}$ NTA column, followed by a HiLoad 16/60 Superdox-200 size exclusion column equilibrated with the stocking buffer (100 mM NaCl, 50 mM Tris–HCl, 10% glycerol, and 2 mM DTT, pH 8.0). The purity of each purified BFPvv mutant was determined using SDS–PAGE and the molecular weight was checked by MALDI-TOF mass spectrometry.

### 2.2. Emission intensity determination

The fluorescence levels of the purified BFPvvD7 and D8 at 0.1 mM in the presence or absence of 0.1 mM NADPH were detected under 352 nm excitation and the emission intensities at 440 nm were recorded using Fluorolog-3 spectrophotometer (Jobin Yvon).

### 2.3. Crystallization

The sample containing 7 mg/ml BFPvvD8 protein and 2 mM NADPH was used in the crystallization screening at 4 °C. Diamond-like crystals appeared in the crystallization drop with the reservoir condition of 20% iso-propanol, 0.1 M HEPES-Na, pH 7.5, and 0.2 M sodium citrate dihydrate after 14 days.

### 2.4. Data collection and structure determination

Before being exposed to the 100 K nitrogen stream, the BFPvvD8_NADPH crystals were soaked in the 20% ethyleneglycol as cryoprotectant. X-ray diffraction data were collected at the National Synchrotron Radiation Research Center (NSRRC) BL13B1 in Taiwan using the ADSC Quantum 315 CCD detector. A data set with resolution up to 2.05 Å was obtained. Data index and integration were done by *HKL2000* (Otwinowski and Minor, 1997). Phase information was obtained by molecular replacement using *Phaser* (McCoy et al., 2005), with the structure of clavulanic acid dehydrogenase (CAD) (PDB code: 2JAP) as the search model. Manual model building was carried out using *Coot* (Emsley and Cowtan, 2004), and data refinement with *Refmac5* (Vagin et al., 2004). The refined model was checked by *PROCHECK* (Laskowski et al., 1993). The data collection and detailed refinement statistics are listed in Table 2.

### 2.5. Fluorescence detection of the BFPvv protein expressed in E. coli

The *lacY* deleted BL21-T1 (DE3) cell was used in protein expression. Bacteria culture of each mutant shared identical conditions of incubation and overexpression to control the protein expression level, which was measured by the protein band intensity in the SDS–PAGE gel. Fluorescence emission of the protein within the *E. coli* cells was detected directly under the excitation of 352 nm.

**Table 1A**
Relative emission intensity of D7 and D8.

| Mutant | Relative brightness |
|---|---|
| D7 | 100.00% ± 1.06% |
| D8 | 126.86% ± 1.39% |

**Table 1B**
Mutations in D7 and D8.

| | D7 | D8 |
|---|---|---|
| Mutations | E40K, L77I, V76A, V83M, S124C, T171M, G176S, E179K | E40K, L77I, V76A, V83M, S124C, T171M, G176S, E179K N58Y, A62T, K199R |

### 2.6. Fluorescent lifetime determination

The same buffer condition and protein concentration as shown in Section 2.2 were used to carry out the fluorescent lifetime determination. The samples were excited at 345 nm by using nF900 (Edinburgh Instruments Ltd.) as the light source, and the fluorescence levels were detected by the M300 monochromator at 440 nm. Data analysis were carried out by using *F900* software program.

### 2.7. Fluorescence detection of mTFP1-BFPvvD8 and EGFP-BFPvvD8

Two possible FRET pairs, mTFP1-BFPvvD8 and EGFP-BFPvvD8, were constructed using the pET46 Ek/LIC cloning vector kit (Novagen). The linker peptide corresponding to the sequence of HVVDDDDK between the C-terminus of mTFP1 or EGFP and the N-terminus of BFPvvD8 in the fused proteins was added into the constructions. The over-expression and purification procedures are similar to that described above (Section 2.1). The fluorescence intensities of the fusion proteins were detected under 352 nm excitation. Fluorescence spectra were recorded using the LS-55 fluorescent spectrometer (PerkinElmer, Waltham, MA) with solutions containing 0.01 mM of fusion proteins with/without 0.015 mM NADPH.

## 3. Results

### 3.1. The purified BFPvvD8 protein showed enhanced emission intensity

Compared to BFPvvD7, D8 contains three extra mutations of N58Y, A62T, and K199R. The result shows that it has the identical excitation/emission wavelength to BFPvvD7, but a further 27%

**Table 2**
Data collection and refinement.

| | BFPvvD8_NADPH complex |
|---|---|
| *Data collection* | |
| Space group | $P4_3$ |
| Unit cell (Å) | a = b = 64.40, c = 262.59 |
| Resolution (Å) | 30–2.05 (2.10–2.05) |
| No. of unique reflections | 66,383 (6413) |
| Redundancy | 6.8 (4.7) |
| Completeness (%) | 99.47 (96.1) |
| Average $I/\sigma$ (I) | 21.4 (2.29) |
| $R_{merge}$ (%) | 7.4 (47.2) |
| *Refinement statistics* | |
| No. of reflections | 62,842 (4431) |
| $R_{work}$ (%) | 18.7 (31.3) |
| $R_{free}$ (%) | 23.4 (32.1) |
| *R.m.s. deviations* | |
| Bond lengths (Å) | 0.011 |
| Bond angles (°) | 1.274 |
| *Average B-factor (Å$^2$)/atoms* | |
| Molecule A | 36.76/1817 |
| Molecule B | 33.21/1643 |
| Molecule C | 33.46/1643 |
| Molecule D | 36.50/1809 |
| NADPH molecule A | 30.13 |
| NADPH molecule B | 33.62 |
| NADPH molecule C | 33.89 |
| NADPH molecule D | 31.74 |
| *Ramachandran plot (%)* | |
| Most favored regions | 90.8 |
| Allowed regions | 9.1 |
| Generously allowed | 0.1 |

* Values in parentheses are for the highest resolution shells.

enhancement in the emission intensity compared to D7 was observed (Table 1A). BFPvvD8 has a total of 11 mutations compare to the WT protein (Table 1B) and has the highest blue fluorescence intensity among the BFPvv mutants so far.

### 3.2. Overall structure of the BFPvvD8_NADPH complex

We solved and refined the complex structure of BFPvvD8_NADPH with resolution up to 2.05 Å to unravel how BFPvvD8 interacts with the chromophore. The crystals with the $P4_3$ *space* group contain four molecules in each asymmetric unit, and each monomer binds one NADPH molecule at the expected active site (Fig. 1A). BFPvvD8 possesses a characteristic of Rossmann fold common to the dinucleotide-binding enzymes (Rossmann et al., 1973, 1974). The overall structure was assigned with three 2-fold axes, *P*, *Q* and *R* accordingly (Fig. 1A), and the structure of BFPvvD8 monomer (chain A) was shown in Fig. 1B. Although the tetrameric BFPvvD8 containing two dimer interfaces along the *P*-axis and the *Q*-axis (*P*-interface and *Q*-interface, respectively) was observed based on the structural information, a mixture of monomeric and dimeric structures in solution was demonstrated by analytical ultra-high centrifugation (AUC) (Fig. 2A). Because of most functional dimeric SDR proteins form the strong four-helix bundles across the *Q*-interfaces (Hoffmann et al., 2007), also a BFPvvD8 double mutant designed to disrupt the interactions between the helix bundles successfully generate a monomeric BFPvvD8 mutant (mBFPvvD8, data not shown), we therefore believe that the *Q*-axis is the biological 2-fold axis of the BFPvvD8 dimer (Figs. 2B and 1A). The diffraction data and coordinates had been deposited to Protein Data Bank with PDB code 3P19.

### 3.3. Active site of the BFPvvD8_NADPH complex structure

The 11 mutations of the BFPvvD8 protein could be roughly sorted into three categories: mutations on the surface, in the core region, and around the NADPH binding cleft (Fig. 3). Although most

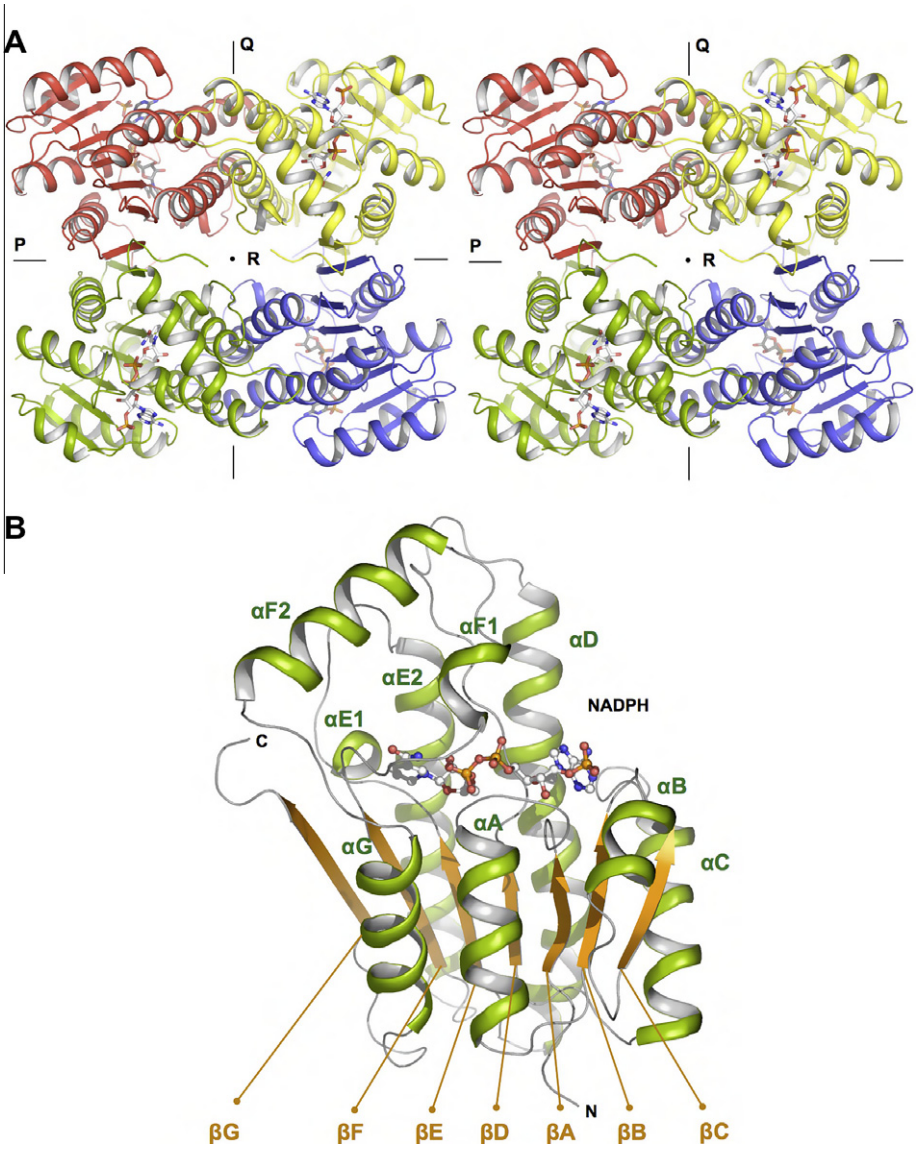


**Fig.1.** Crystal structure of the BFPvvD8_NADPH complex. (A) The overall structure of BFPvvD8_NADPH. There are four molecules in an asymmetric unit represented as ribbon diagrams in four different colors. The overall structure can be assigned with three 2-fold axes, *P*, *Q* and *R* following the definition of Rossmann, and it possesses a characteristic Rossmann fold common to the dinucleotide-binding enzymes. In the solved complex structure, each monomer binds one NADPH molecule at the expected active site, the bound NADPH is shown as stick. (B) The monomer of BFPvvD8_NADPH (chain A). The secondary structure was checked and confirmed by *PROCHECK* before designation. The NADPH binding pattern is also presented.

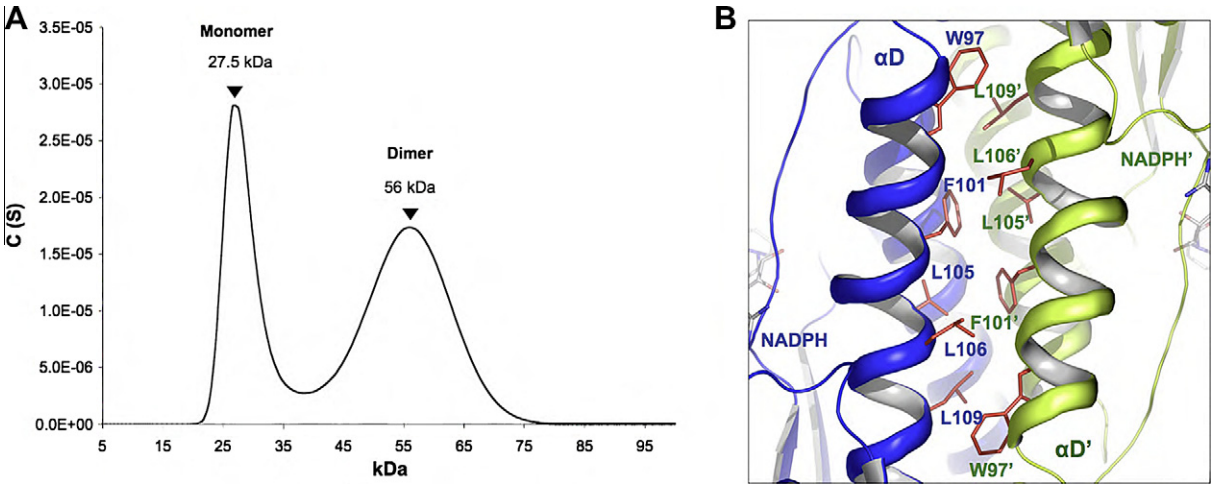


**Fig.2.** (A) The dimeric structure (D8) in solution revealed by analytical ultra centrifugation (AUC) experiment. The solved crystallographic structure is consisted of four molecules, but the result of AUC analysis shows the existence of monomer and dimer of BFPvv in the solution. The calculated molecular weight and the theoretical state of monomer or dimer is labeled. (B) The interactions of the BFPvv dimer interface. The interface along the *Q*-axis was established by an intermolecular four-helix bundle and was stabilized by the hydrophobic interactions between αD and αE with its *Q*-axis symmetrical partner. The residues involved in the interactions are showed in sticks. It was believed to be the stable dimeric form of BFPvv in solution along *Q*-axis, since the double mutation W97K and F101K generated monomeric BFPvvD8 with no fluorescent activity (data not shown).

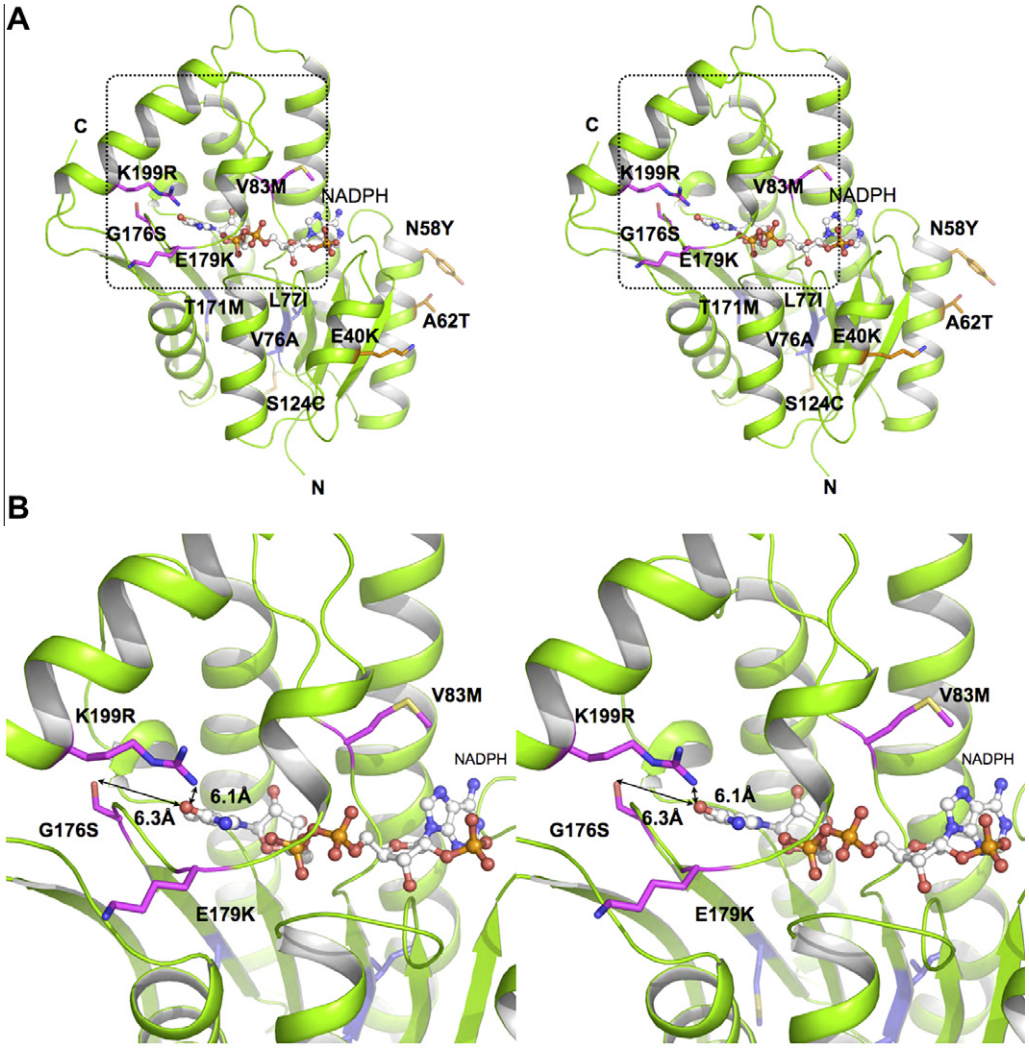


**Fig.3.** (A) Stereo view of the BFPvvD8_NADPH monomer (chain A). The BFPvvD8 protein is represented as ribbon diagram and the bound NADPH molecule is depicted as ball-and-stick. Side chains of all 11 mutations are shown as sticks, and sorted into three categories: mutation on the surface, the core region, and around the NADPH binding cleft, colored with yellow, blue, and magenta, respectively. The dashed rectangular box area around the NADPH is enlarged in (B).

of the mutations were supposed to provide contributions to the enhancement of emission intensity; however, we failed to observe any direct interactions between the side-chains of these mutations to NADPH from the interaction profile assigned by *LIGPLOT* (Wallace et al., 1995) (Fig. S1).

Intriguingly, when comparing the BFPvvD8_NADPH complex structure with a homologous structure, CAD (PDB code: 2JAP, the r.m.s deviation (r.m.s.d) value of 1.1 Å with 236 Cα atoms superimposed), we found that the carbonyl group of Gly186 in CAD points toward the carbonyl group of NADPH (O7), with a distance of 3.74 Å, whereas in our BFPvvD8 structure, the same carbonyl group of the aligned Ser176 (Gly mutated to Ser) turns to the opposite direction, and the main chain nitrogen atom flips up toward the same carbonyl group (O7) of NADPH (Fig. 4A) with a distance of 3.37 Å between them (Fig. 5A). Similar result could also be observed in the superimposition of BFPvvD8 to the BFPvvWT modeling structures, one was predicted by *SWISS-MODEL* (Arnold et al., 2006) and the other was generated through energy minimization using *CNS* program (Brunger et al., 1998) of the manual adjusted BFPvvD8_NADPH structure (Fig. S2A and B). This S176 is mutated from the highly conserved glycine residue in the "PG box" in most of the SDR family (Ghosh and Vihko, 2001). In addition to CAD, we compared our structure to several homologous SDR structures with their r.m.s.d (Cα atoms) around 1.1–2.3 Å. It was suggested that this main chain torsion in D8 is unique among these homologues structures (Figs. 4B and 4C), which makes N of A177 pointing toward carbonyl O7 of nicotinamide with the distances of 3.37 Å in chains A and D, and 3.00 Å in chains B and C, which are acceptable distances for interactions (Fig. 5A). The $\psi/\phi$ for S176-A177 in D8 (chain A) is 143°/58°, and −163°/−50° in the aligned position of CAD. Unambiguous density map of this PG-box neighboring region and the residues involved in the hydrophobic pocket are shown in Fig. S3A and B.

### 3.4. Emission intensities of BFPvvWT, BFPvv(G176S), BFPvv(G176A), and BFPvvD8

To further validate the influence of the interactions between Gly176 and NADPH in terms of the fluorescent properties, we constructed the mutation of G176S on the WT BFPvv protein. In the

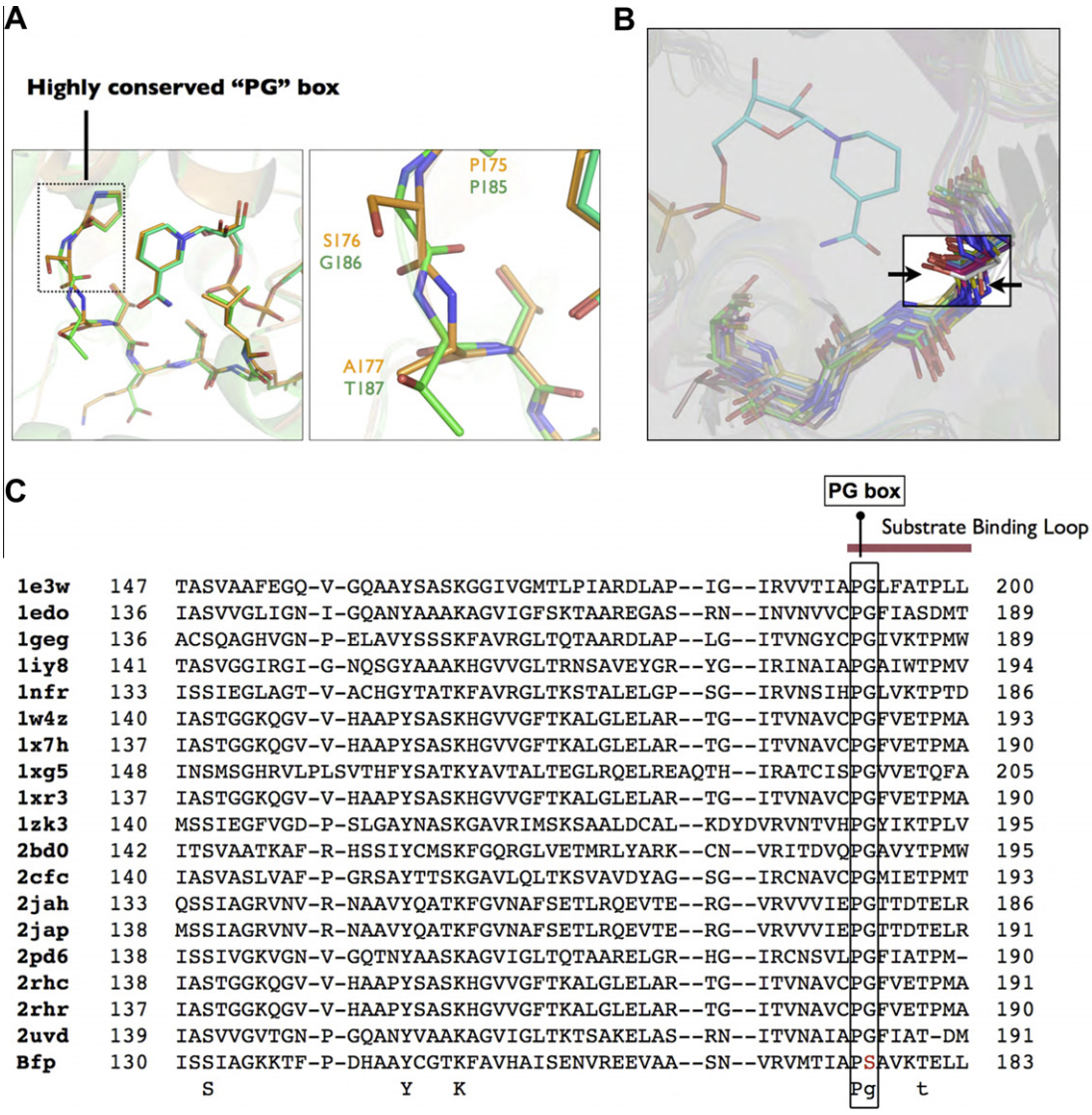


**Fig.4.** (A) Superimposition of BFPvvD8_NADPH and a homologous structure, clavulanic acid dehydrogenase (CAD, PDB code: 2JAP) of the conserved "PG box". BFPvvD8 is colored in orange, and CAD is in green color. (B) Structural alignment of the SDR family at the NADPH binding site. The box indicates the conserved "PG box" in most members of the SDR family. Arrow emphasizes that the main chain flip caused by a non-Gly substitution of Gly residue in the PG box. The conserved "PG box" was also highlighted in the structural based sequence alignment of these homologues SDR proteins shown in (C).

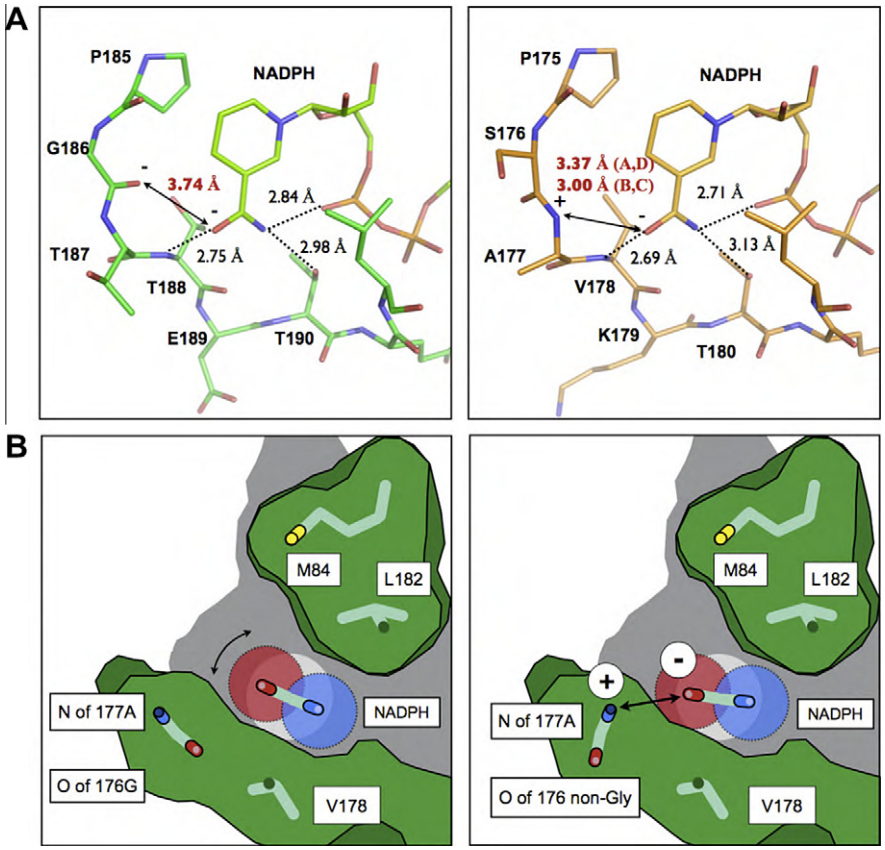


**Fig.5.** The proposed status of the Gly (left) or non-Gly (right) residue corresponding to the position 176 of BFPvv. (A) Interaction of O7 of nicotinamide to the neighboring charged atoms. Left: in CAD (PDB code: 2JAP, chain A), the carbonyl group of Gly186 points toward the carboxyl group of NADPH (O7). Right: in BFPvv (chain A), the Gly176 residue was mutated into a non-Gly residue (serine residue presented here), the nitrogen atom of Ala177 thus flipped toward O7 of NADPH. (B) Cartoon diagram illustrates the proposed status of the Gly (Left) or non-Gly (Right) residue at the position 176 of BFPvv.

fluorescence assay of the expressed protein in *E. coli*, emission of the single point mutant BFPvv(G176S) showed a 2-fold increase comparing to wild-type BFPvv, which is consistent to the previous report (Polizzi et al., 2007). Similarly, another single mutant, BFPvv(G176A), produced approximately the same level of emission intensity as BFPvv(G176S) (Table 3). Notably, we observed a blue-shifted emission peak of BFPvv(G176A) and BFPvv(G176S); the emission peak of wild-type BFPvv is around 450 nm, whereas the emission peak of both single mutants is 440 nm, similar to that of BFPvvD7 and BFPvvD8, consistent in several rounds of detection (Fig. 6).

### 3.5. The fluorescence lifetime of BFPvv mutants

The purified proteins were used to measure the fluorescence lifetime of each mutant to see how mutation of G176 would alter the chromophore properties of NADPH in various BFPvv proteins. According to our data, NADPH alone showed a very short fluorescent lifetime, 0.43 ns, in the buffer; however, the lifetime could be prolonged to 4.29 ns when it is bound to WT BFPvv (Table 3).

**Table 3**
Relative emission intensity of BFPvv proteins.

| Mutant | Relative brightness |
|---|---|
| WT | 25.28% ± 1.81% |
| WT176S | 45.31% ± 1.07% |
| WT176A | 54.58% ± 1.36% |
| D8 | 100.00% ± 2.87% |

An even longer lifetime of 7.26 ns could be observed while incubating NADPH with BFPvv(G176S), an approximately similar lifetime to BFPvvD8_NADPH. Thus, the G176S mutation seems to play a distinct role in affecting the fluorescence lifetime in BFPvvD8 (Table 4).

### 3.6. Monomeric SDR enzyme hCBR1 enhances NADPH fluorescence similar to BFPvvWT

The comparison of the fluorescent spectrum of NADPH alone, BFPvvWT, BFPvv mutants, and the monomeric SDR protein human carbonyl reductase 1 (hCBR1) was shown in Fig. 6. The hCBR1 protein, which belongs to the human SDR family with known structure, could also reinforce the fluorescence of NADPH by 3.2 folds, similar to that of BFPvvWT (4.8 folds). While NADPH binds to both WT proteins (BFPvv and hCBR1), the emission peaks showed a significant blue shifting comparing to that of NADPH alone (from 460 to 450 nm). The result implied that other SDR proteins might be considered as potential targets in the NADPH-dependent BFP development.

### 3.7. Energy transfers in mTFP1-BFPvvD8 and EGFP-BFPvvD8

The excitation and emission wavelengths of EGFP and mTFP1 were 488 and 510 nm, 462 and 493 nm, respectively. Under 352 nm of exposure, the emission spectra of both fusion proteins without NADPH were relatively weak (Fig. 7C, dashed lines). After adding NADPH to each sample, the emission of EGFP and mTFP1 (510 and 493 nm, respectively) rose significantly (Fig. 7C, solid

lines). Since BFPvvD8 only has emission peak at 440 nm (Fig. S4B), the clear observations of green fluorescence from the fusion proteins suggest that energy emits from BFPvvD8 at 440 nm could successfully transfer to both fused GFPs which then emit longer wavelength green fluorescence.

## 4. Discussion

In the previous research, BFPvvD7 had been shown to have enhanced fluorescence intensity than wild-type BFPvv (Chang et al., 2004). Without the structural information, the reason for this remained ambiguous. According to our BFPvvD8_NADPH complex structure, N of A177 points toward carbonyl O7 of nicotinamide, which is different from that seen in several other homologous SDR structures. The distance between N of the peptide bond to O7 of NADPH is close enough for hydrogen bonding interaction (Fig. 5A). Usually, O7 is considered as partially negatively-charged; in contrast, N is considered as partially positively-charged (~40%). This observed charge-charge interaction is likely to further restrict the torsion of the C—C single bond between the reduced nicotinamide ring and the amide group, which theoretically increases the rigidity of the structure of nicotinamide and hence decreases the non-radiative decay. This hypothesis could be further supported by the detection of fluorescence lifetime, a parameter to represent the summation of the rate of radiative and non-radiative decay. BFPvv(G176S)_NADPH showed a longer lifetime than wild-type BFPvv_NADPH (Table 4). With the radiative decay rate of a chromophore, i.e., NADPH remains constant; the non-radiative decay rate was significantly decreased by the single amino acid substitution of Gly176 to Ser. Also, the aforementioned N–O7 interaction adjacent to the bound chromophore is likely to be caused by the single mutation at G176 since no other additional direct interaction to nicotinamide could be observed after S176 substitution in the BFPvvD8_NADPH structure. Moreover, a single mutation (G176A) of WT BFPvv also increased the emission to approximately the same level. Substitution of a Gly to a non-Gly residue may impact the neighboring structure in order to lower the stereo hindrance. Generally speaking, Gly could adopt a large range of dihedral angles in a polypeptide chain. Some point mutations on the position 176 of BFPvvD8, e.g., G176T, G176E and G176K, showed no influence to the emission intensities of BFPvvD8 (Table S2), further supports this hypothesis. Taken together, we suggest that G176S is responsible for the main-chain torsional change, which decreases the non-radiative decay via a charge–charge interaction between N of A177 and O7 of nicotinamide (Fig. 5B). We could also eliminate the possibility that other 10 mutation sites might have contributed to the non-radiative decay, as these mutations in BFPvvD8 did not significantly influence the fluorescence lifetime (7.03 ns).

Structural alignment through DALI server showed that the overall structure of BFPvvD8 shares high similarity with many SDR members despite their low sequence identity (30%), the r.m.s.d. with their Cα carbons compared are all below 2.1 Å. Interestingly, this G176 is in a conserved region called "PG" box among the SDR family (Ghosh and Vihko, 2001). Because of all these similar foldings between BFPvv D8 and other SDR proteins, the mutations on the Gly residue of the PG box to other non-Gly amino acids might give rise to the idea of increasing fluorescence among the SDR family upon NADPH binding. Although BFPvv(G176S) and BFPvvD8

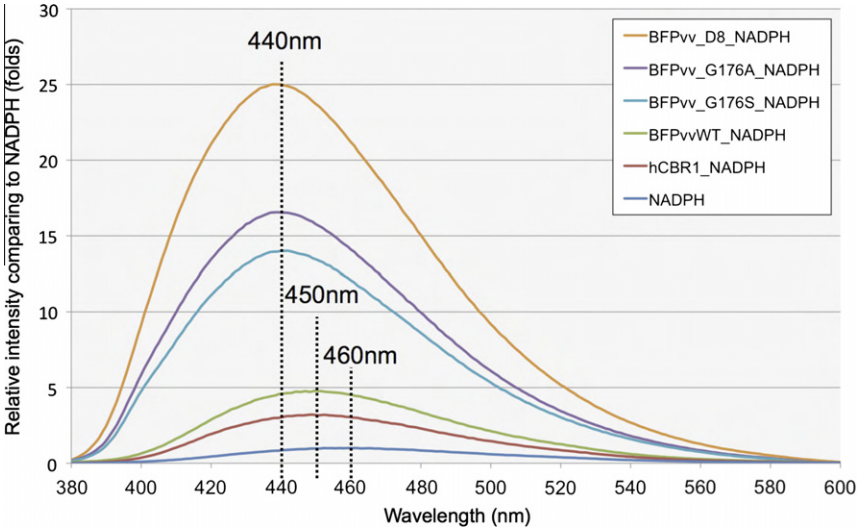


**Fig.6.** Emission spectra of NADPH alone, hCBR1, BFPvv 176 mutants and BFPvvD8. The monomeric SDR protein, hCBR1, has an enhanced emission upon NADPH binding, similar to the BFPvvWT. The emission intensities of hCBR1 and BFPvvWT are 3.2 and 4.8 folds comparing to that of NADPH alone, respectively. A blue-shifted emission spectrum (emission peak from 460 to 450 nm) whilst NADPH binding to hCBR1 was also observed. In the BFPvv 176 mutants (G176A, G176S and D8), the emission peak were further shifted to the wavelength of 440 nm.

**Table 4**
Fluorescence lifetime of NADPH complexed BFPvv proteins.

| Sample | Short lifetime | | Long lifetime | | Very long lifetime | | |
|---|---|---|---|---|---|---|---|
| | $\tau$ (ns) | $f$ (%) | $\tau$ (ns) | $f$ (%) | $\tau$ (ns) | $f$ (%) | $x^2$ |
| NADPH | 0.43 | 100 | – | – | – | – | 1.015 |
| WT + NADPH | – | – | 4.29 | 100 | – | – | 1.000 |
| G176S + NADPH | 0.42 | 20 | – | – | 7.26 | 80 | 1.074 |
| D7 + NADPH | 0.57 | 21 | – | – | 7.60 | 79 | 1.007 |
| D8 + NADPH | 0.50 | 17 | – | – | 7.03 | 83 | 0.962 |

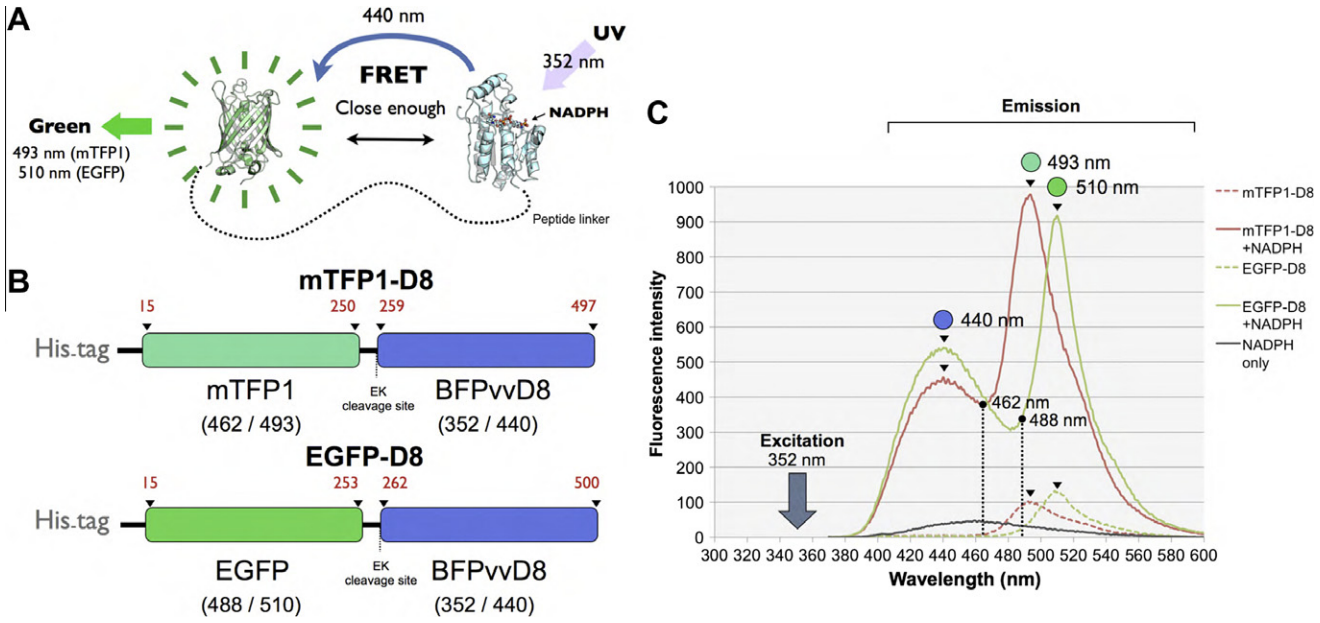


**Fig.7.** BFPvvD8 serves as a FRET donor and is suitable for the FRET-based biosensor design. (A) The concept in designing the BFPvvD8-GFP FRET pair. (B) The fusion proteins of the two BFPvvD8-GFP FRET pairs. Two GFP-like FPs, EGFP and mTFP1, with excitation and emission wavelengths of 488 and 510 nm, 462 and 493 nm, respectively, were fused to the N-terminal of BFPvvD8 using the pET46 Ek/LIC cloning vector kit (Novagen). The red number indicated the position in the fused protein. (C) The energy transfers between the BFPvvD8 and GFPs in the fusion proteins were observed. The BFPvvD8-GFP fusion proteins were excited at 352 nm, and the emission fluorescence intensities at higher wavelengths were recorded. The solid lines represent the fluorescence intensities of the fusion proteins with NADPH, whereas the dashed lines were the results of fusion proteins only.

exhibited similar fluorescence lifetime, the emission intensity of BFPvvD8 is obviously higher than BFPvv(G176S) (Table 3). Therefore, remaining mutations contribute to the fluorescence enhancement in somehow a different path from that of BFPvv(G176S).

When chromophores are bound to proteins, proteins could not only increase the rigidity of the chromophores, but also shield them from the contact of the solvent, which could eliminate the energy dissipation through fluorescence. The ITC results show that the association constants, Ka, measuring the binding affinities of NADPH to wild-type BFPvv and BFPvvD8, were similar (Fig. S5 and Table S1). This suggests that the fourfold enhancement of fluorescence intensity is not due to the increased affinity. Interestingly, we found different circular dichroism spectra between WT and WT_NADPH, but not between D8 and D8_NADPH (Fig. S6). These results may imply that the binding process of NADPH to WT BFPvv and BFPvvD8 are through very different procedures, which may involve many attractive forces such as hydrogen bonds, van der Waal interactions and the hydrophobic interactions. The difference in the binding profiles could possibly donate different environmental dynamics to the bound NADPH, altering the shielding ability of this chromophore. For example, binding through the more dynamic procedure would probably result in a less shielded NADPH, which might decrease the energy released via fluorescence. Albeit it is not clear about how exactly the binding process could affect the fluorescence of NADPH, binding dynamic is one possibility underlying the enhanced fluorescence in BFPvvD8. Increasing the environmental hydrophobicity and rigidity, which can decrease non-fluorescent energy dissipation of the chromophore, thus enhance the fluorescence intensity. The similar fluorescent characteristic was also preliminarily found in another monomeric SDR protein, i.e., hCBR1, upon NADPH binding. A 3.2 fold increase in the intensity of fluorescence spectrum accompanied with the blue-shifted emission was observed in hCBR1_NADPH mixture comparing to NADPH alone (Fig. 6). We therefore believed that the SDR proteins, which are all NADPH-binding, and share the common fold of the global conformations, are potentially engineered into proteins that can emit brighter fluorescence through our structure-function strategy, making them more preferable to applications.

Importantly, BFPvvD8 can emit fluorescence in an oxygen-limited condition, whereas EGFP cannot (data not shown). Our result is corroborated with the previous study of FMN-based FPs (Drepper et al., 2007). As a parallel system of fluorescent protein, the application of BFPvvD8 being as the FRET donor with GFP-like acceptors was assessed. The energy transmission in EGFP-BFPvvD8 and mTFP1-BFPvvD8 via FRET were successfully observed (Fig. 7) using the absorption and excitation/emission spectra of BFPvvD8_NADPH, mTFP1-BFPvvD8_NADPH, and mTFP1-BFPvvD8_NADPH as reference (Fig. S4A and B). Generally, monomeric FPs would be better for the usage of FRET-based biosensors design, however, some weak-dimer form of FPs, e.g., GFP-derived FPs, could also be considered in the FRET-based biosensor systems (Piston and Kremers, 2007). BFPvvD8 exists as a mixture of monomer and dimer in free solution, which was revealed by the AUC analysis (Fig. 3A), and the observed FRET phenomena between the BFPvvD8 and two of the GFPs suggests that the BPFvvD8 is potentially applicable in the designs of FRET-based biosensors with GFP-like acceptors. Also, with the characterization of NADPH-binding/oxygen-limited emitting abilities, BFPvvD8 may provide alternative options in the FRET-based reporter design, such as NADPH or oxygen biosensors after optimized.

In summary, NADPH serves as the source of reducing power in living organisms and discovering NADPH-based fluorescent proteins turns this ubiquitous molecule into an intrinsic fluorescent probe. Here we discovered a new mutated blue fluorescence protein, BFPvvD8, with enhanced emission intensity grater than previously described D7. The improvement in the emission intensity expands the applicability as a fluorescent protein itself, or as a FRET donor. To elucidate the rationale behind the emissive D8, we solved the crystal structure in complex with NADPH, which could serve as the foundation of further structure-based protein engineering. This structural information and the explanation presented here provide more insight into our knowledge of other

SDR family proteins akin to the unique BFPvv fluorescence protein. The greatly enhanced fluorescence of BFPvvD8 provides valuable design information of fluorescent protein variants as a well-suited tool for multicolor imaging and other applications in biology.

## Acknowledgments

We would like to acknowledge Prof. Pi-Tai Chou (Department of Chemistry, National Taiwan University) for his suggestions and supports in fluorescent lifetime determination, and National Synchrotron Radiation Research Center for their supports for x-ray data collections. We also thank the Biophysics Core Facility (BCF) of the Scientific Instrument Center, Academia Sinica for the ITC instrument. The Protein Crystallography Facility of National Synchrotron Radiation Research Center is supported by the National Research Program for Genomic Medicine. Mass spectrometry analyses were performed by the Core Facilities for Proteomics Research located at the Institute of Biological Chemistry, Academia Sinica. This work was supported by Academia Sinica and Core Facility for Protein Production and X-Ray Structural Analysis (Grant NSC97-3112-B-001-035-B4) to A.H.-J. Wang. C. H. Pai is grateful for the Postdoctoral Fellowship from Academia Sinica, Taiwan.

## Appendix A. Supplementary data

Supplementary data associated with this article can be found, in the online version, at doi:10.1016/j.jsb.2011.02.010.

## References

Arnold, K., Bordoli, L., Kopp, J., Schwede, T., 2006. The SWISS-MODEL workspace: a web-based environment for protein structure homology modelling. Bioinformatics 22, 195–201.

Brejc, K., Sixma, T.K., Kitts, P.A., Kain, S.R., Tsien, R.Y., Ormo, M., Remington, S.J., 1997. Structural basis for dual excitation and photoisomerization of the Aequorea victoria green fluorescent protein. Proc. Nat. Acad. Sci. USA 94, 2306–2311.

Brunger, A.T., Adams, P.D., Clore, G.M., DeLano, W.L., Gros, P., Grosse-Kunstleve, R.W., Jiang, J.S., Kuszewski, J., Nilges, M., Pannu, N.S., Read, R.J., Rice, L.M., Simonson, T., Warren, G.L., 1998. Crystallography and NMR system: a new software suite for macromolecular structure determination. Acta Crystallogr. D Biol. Crystallogr. 54, 905–921.

Chang, C.C., Chuang, Y.C., Chang, M.C., 2004. Fluorescent intensity of a novel NADPH-binding protein of Vibrio vulnificus can be improved by directed evolution. Biochem. Biophys. Res. Commun. 322, 303–309.

Drepper, T., Eggert, T., Circolone, F., Heck, A., Krauss, U., Guterl, J.K., Wendorff, M., Losi, A., Gartner, W., Jaeger, K.E., 2007. Reporter proteins for in vivo fluorescence without oxygen. Nat. Biotechnol. 25, 443–445.

Emsley, P., Cowtan, K., 2004. Coot: model-building tools for molecular graphics. Acta Crystallogr. D Biol. Crystallogr. 60, 2126–2132.

Ghosh, D., Vihko, P., 2001. Molecular mechanisms of estrogen recognition and 17-keto reduction by human 17b-hydroxysteroid dehydrogenase 1. Chem. Biol. Interact. 130–132, 637–650.

Heim, R., Prasher, D.C., Tsien, R.Y., 1994. Wavelength mutations and posttranslational autoxidation of green fluorescent protein. Proc. Nat. Acad. Sci. USA 91, 12501–12504.

Hoffmann, F., Sotriffer, C., Evers, A., Xiong, G., Maser, E., 2007. Understanding oligomerization in 3alpha-hydroxysteroid dehydrogenase/carbonyl reductase from Comamonas testosteroni: an in silicon approach and evidence for an active protein. J. Biotechnol. 129, 131–139.

Laskowski, R.A., MacArthur, M.W., Moss, D.S., Thornton, J.M., 1993. PROCHECK: a program to check the stereochemical quality of protein structures. J. Appl. Crystallogr. 26, 283–291.

McCoy, A.J., Grosse-Kunstleve, R.W., Storoni, L.C., Read, R.J., 2005. Likelihood-enhanced fast translation functions. Acta Crystallogr. D Biol. Crystallogr. 61, 458–464.

Otwinowski, Z., Minor, W., 1997. Processing of X-ray diffraction data collected in oscillation mode. Macromol. Crystallogr. Part A 276, 307–326.

Piston, D.W., Kremers, G.J., 2007. Fluorescent protein FRET: the good, the bad and the ugly. Trends Biochem. Sci. 32, 407–414.

Polizzi, K.M., Moore, D.A., Bommarius, A.S., 2007. A short-chain dehydrogenase/reductase from *Vibrio vulnificus* with both blue fluorescence and oxidoreductase activity. Chem. Commun. (Camb), 1843–1845.

Rossmann, M.G., Moras, D., Olsen, K.W., 1974. Chemical and biological evolution of nucleotide-binding protein. Nature 250, 194–199.

Rossmann, M.G., Adams, M.J., Buehner, M., Ford, G.C., Hackert, M.L., Liljas, A., Rao, S.T., Banaszak, L.J., Hill, E., Tsernoglou, D., Webb, L., 1973. Molecular symmetry axes and subunit interfaces in certain dehydrogenases. J. Mol. Biol. 76, 533–537.

Shu, X., Royant, A., Lin, M.Z., Aguilera, T.A., Lev-Ram, V., Steinbach, P.A., Tsien, R.Y., 2009. Mammalian expression of infrared fluorescent proteins engineered from a bacterial phytochrome. Science 324, 804–807.

Su, J.H., Chuang, Y.C., Tsai, Y.C., Chang, M.C., 2001. Cloning and characterization of a blue fluorescent protein from *Vibrio vulnificus*. Biochem. Biophys. Res. Commun. 287, 359–365.

Vagin, A.A., Steiner, R.A., Lebedev, A.A., Potterton, L., McNicholas, S., Long, F., Murshudov, G.N., 2004. REFMAC5 dictionary: organization of prior chemical knowledge and guidelines for its use. Acta Crystallogr. D Biol. Crystallogr. 60, 2184–2195.

Wallace, A.C., Laskowski, R.A., Thornton, J.M., 1995. LIGPLOT: a program to generate schematic diagrams of protein–ligand interactions. Protein Eng. 8, 127–134.